Can System Truncation Speed up Ligand-Binding Calculations with Periodic Free-Energy Simulations?

Manzoni, Francesco; Uranga, Jon; Genheden, Samuel; Ryde, Ulf

Published in:
Journal of Chemical Information and Modeling

DOI:
10.1021/acs.jcim.7b00324

2017

Document Version:
Early version, also known as pre-print

Can System Truncation Speed up Ligand-Binding Calculations with Periodic Free-Energy Simulations?

Francesco Manzoni, Jon Uranga,[a] Samuel Genheden,[b] Ulf Ryde *

Department of Theoretical Chemistry, Lund University, Chemical Centre, P. O. Box 124, SE-221 00 Lund, Sweden

[a] Current address: Kimika Fakultatea, Euskal Herriko Unibertsitatea (UPV/EHU) and Donostia International Physics Center (DIPC), P.K. 1072, 20080, Donostia, Euskadi, Spain

[b] Current address: Department of Chemistry and Molecular Biology, Box 462, University of Gothenburg, SE-405 30 Göteborg, Sweden

Correspondence to Ulf Ryde, E-mail: Ulf.Ryde@teokem.lu.se,
Tel: +46 – 46 2224502, Fax: +46 – 46 2228648

This article is dedicated to the memory of Francesco Manzoni, who died from a heart attack on March 12th at the age of 27.

Abstract

We have investigated whether alchemical free-energy perturbation calculations of relative binding energies can be sped up by simulating a truncated protein. Previous studies with spherical non-periodic systems showed that the number of simulated atoms could be reduced by a factor of 26 without affecting the calculated binding free energies by more than 0.5 kJ/mol on average (Genheden, S. & Ryde, U., J. Chem. Theory Comput., 2012, 8, 1449), leading to 63-fold decrease in the time consumption. However, such simulations are rather slow, owing to the need of a large cut-off radius for the non-bonded interactions. Periodic simulations with the electrostatics treated by Ewald summation are much faster. Therefore, we have investigated if a similar speed-up can be obtained also for periodic simulations. Unfortunately, our results show that it is harder to truncate periodic systems and that the truncation errors are larger for these systems. In particular, residues need to be removed from the calculations, which means that atoms have to be restrained to avoid that they move in an unrealistic manner. The results strongly depend on the strength on this restraint. For the binding of seven ligands to dihydrofolate reductase and ten inhibitors of blood-clotting factor Xa, the best results are obtained with a small restraining force constant. However, the truncation errors were still significant (e.g. 1.5–2.9 kJ/mol at a truncation radius of 10 Å). Moreover, the gain in computer time was only modest. On the other hand, if the snapshots are truncated *after* the MD simulations, the truncation errors are small (below 0.9 kJ/mol even for a truncation radius of 10 Å). This indicates that post-processing with a more accurate energy function (e.g. with quantum chemistry) on truncated snapshots may be a viable approach.

Key Words: Free-energy perturbation, ligand binding, system truncation, factor Xa, dihydrofolate reductase.

Introduction

One of the largest challenges for computational biochemistry is to estimate the free energy for the binding of a ligand to a macromolecule, e.g. the binding of a drug candidate to its receptor. Consequently, many methods have been suggested with this aim, ranging from simple scoring functions to strict alchemical free-energy perturbation (FEP) methods, such as exponential averaging, thermodynamic integration, Bennett acceptance ratio (BAR), and related methods.[1–3] In the latter methods, the difference in binding free-energy between two ligands is obtained by sampling the difference in potential energy during a molecular dynamics (MD) or Monte Carlo simulation. Unfortunately, the result converges only for small differences between the ligands, so the calculations need to be divided into many small steps, in which one ligand is slowly transformed into the other through a number of intermediate non-physical (alchemical) states. Therefore, these methods become very time-consuming. Still, they have successfully been used to help the design of new drugs in several cases[4,5] and they have been shown to give a mean absolute error of 4–6 kJ/mol compared to experimental data in several recent large-scale test studies.[6–9]

To make the FEP methods more attractive for general applications in real drug-development project, it is of great interest to speed up the calculations. For example, we have studied whether the simulation time and number of intermediate states can be reduced without affecting the accuracy of the method.[10] Moreover, we have shown for the binding of ten inhibitors to the blood-clotting factor Xa (fXa) that the simulated system can be reduced from around 39 000 to 1500 atoms without affecting the calculated affinities by more than 0.5 kJ/mol on average (maximum change 1.4 kJ/mol), reducing the computational time by a factor of 63.[11] These calculations were performed on spherical systems with the Q software.[12] Unfortunately, such calculations require a large cut-off radii for the electrostatic interactions. More effective simulations can be performed with periodic systems and the electrostatics treated with Ewald summation.[13] In fact, simulations with the truncated system were only ~4 times faster than simulations with the full system and Ewald summation, despite that only 1/26 of the atoms were considered[11] (although this is partly an effect of the fact that the Amber software is more optimised for speed than the Q software).

Therefore, it is interesting to see whether similar reductions of the simulated systems are possible also in periodic simulations. This is not evident, because artefacts caused by the enforced periodicity becomes more pronounced the smaller the simulated system is. We try such an approach in this article, employing the same test system as in our previous articles,[10,11] viz. the relative affinities of eight pairs of ligands for fXa.[14] We also study the binding of seven 2,4-diaminopyrimidine ligands to dihydrofolate reductase (DHFR),[15,16] which has been considered in several previous computational studies.[7,17]

Methods

Structures

The seven 2,4-diaminopyrimidine ligands of DHFR are shown in Figure 1, together with the six considered transformations. The calculations were based on the crystal structure with PDB code 1J3I (2.33 Å resolution) with a similar ligand.[18] The simulations were set up in the same way as in our previous calculations of this system.[7]

The ten 3-amidinobenzyl-1*H*-indole-2-carboxamide inhibitors of fXa considered in this study are shown in Figure 2. They are named according to their numbers in the original experimental study.[14] The preparation of these ligands has been described before.[7,10,11] All calculations were started from the crystal structure of fXa in complex with ligand 125 (PDB code 1LPK, 2.3 Å resolution).[14] The crystal structure involves two conformations for one of the amidino groups of the

ligand, but only a single conformation of the ligand was studied here (the A conformation) because our previous study did not show any difference between the affinities of the two alternative conformations.[10] Our aim is to compare simulations with truncated systems with those of the full protein and for such comparison it is enough to study one conformation (comparison with experimental data is of secondary interest).

The preparation of the proteins has also been described before:[7,10,11,19] All Arg and Lys residues were supposed to have a positive charge and the Glu and Asp residues were assumed to have a negative charge. For fXa, His57 and 83 were protonated on the $N^{\delta 1}$ atom, His91, 145, and 199 on the $N^{\varepsilon 2}$ atom, and His13 on both atoms. DHFR does not contain any His residues. To be comparable to our previous studies,[7,10,11,19] DHFR was described with the Amber 99SB force field,[20] whereas fXa was described by the Amber 99 force field.[21] All ligands were treated with the general Amber force field,[22] with charges derived by the restrained electrostatic potential (RESP) method[23] using potentials calculated at the Hartree–Fock 6-31G* level and sampled with the Merz–Kollman scheme.[24]

The protein–ligand complexes and the free ligands were solvated in a truncated octahedral box of TIP3P waters[25] that extended at least 8 Å from the solute using the tleap module of the Amber 11 suite of programs.[26] Truncated systems were obtained by deleting all residues more than a certain distance (r) from the ligand; distances of 25, 20, 15, and 10 Å were employed (and also 35 and 30 Å for the larger fXa protein). The systems were truncated before they were solvated, so the size of the periodic box also decreased for the truncated systems. To avoid unphysical movements of the remaining atoms, heavy atoms between r and $r - 4$ Å were included in the calculations, but they were restrained towards the starting structure with a force constant (k_{res}) of either 4184 or 1.3 kJ/mol/Å^2. An example of the truncations is shown in Figure 3. The truncated residues retained the same charges as in the full system and no capping groups were employed.

Molecular dynamics simulations

The MD simulations were performed with the sander module of Amber 11 or 12.[26,27] The temperature was kept constant at 300 K using a Langevin thermostat[28] with a collision frequency of 2.0 ps^{-1}, and the pressure was kept constant at 1 atm using a weak-coupling isotropic algorithm[29] with a relaxation time of 1 ps. Particle-mesh Ewald summation[13] with a fourth-order B spline interpolation and a tolerance of 10^{-5} was used to calculate electrostatic energies and forces. The cut-off for the Lennard-Jones interactions was set to 8 Å and the non-bonded pair list was updated every 50 fs. The SHAKE algorithm[30] was used to constrain bonds involving hydrogen atoms so that a 2 fs time step could be used.

The FEP calculations were performed in the following way: The system at each λ value was minimized for 500 cycles of steepest descent, with all atoms except water molecules and hydrogen atoms restrained to their start position with a force constant of 418 kJ/mol/Å^2. This was followed by a 20 ps constant-pressure simulation, using the same constraints, and a 200 ps constant-pressure simulation without any restraints. Finally, a 2 ns constant-pressure production run was performed, during which coordinates and energies were sampled every 10 ps.

Free-energy calculations

We have calculated the relative free energy of six and eight inhibitor transformations for DHFR and fXa, respectively, as is described in Figures 1 and 2, using a thermodynamic cycle that involves the conversion of one ligand (L_1) to the other (L_2) both in the protein binding site and in solution.[10,32] The free energies of the transformations were calculated using the multi-state Bennett acceptance ratio (MBAR) approach,[33] but other methods, including BAR,[34] exponential averaging,[35] and thermodynamic integration,[36] were also considered. All these free-energy

differences were calculated with the PYMBAR software.[33] We employed the single transformation-approach[10,11] in which both electrostatic and van der Waals interactions are modified in the same step. The calculations employed soft-core versions of both the van der Waals and Coulomb potentials, which have been calibrated for this type of calculations with the AMBER software.[37,38]

To improve the convergence of the free-energy difference, the transformation $L_1 \rightarrow L_2$ was divided into several small steps, involving intermediate states, defined by the potential energy $V(\lambda) = (1 - \lambda)\, V_0 + \lambda V_1$, where V_0 and V_1 are the potential energies of the L_1 and L_2 states, respectively. Eleven λ values were used (0.05, 0.1, 0.2, 0.3, 0.4, 0.5, 0.6, 0.7, 0.8, 0.9, and 0.95). Data for $\lambda = 0$ and 1 were obtained by a linear interpolation using the two closest values. In all calculations, we use a dual-topology scheme with two sets of coordinates for the atoms that differ between L_1 and L_2.

To improve the precision of the results, DHFR simulations were rerun with the pmemd module of the AMBER 16 software,[39] allowing for single-topology simulations also at the $\lambda = 0$ and 1 endpoints.[40] The final two MD simulations were elongated to 1 ns equilibration and 5 ns production, and energies were sampled every 1 ps for the MBAR free-energy calculations. These are the DHFR results discussed throughout the text.

Error estimates

All reported uncertainties are standard errors of the mean (standard deviations divided by the square root of the number of samples). The uncertainty of the MBAR free energies calculated at each λ value was estimated by bootstrapping using the PYMBAR software[33] and the total uncertainty was obtained by error propagation.

The performance of the free-energy estimates was quantified by the mean absolute deviation (MAD), the root-mean-squared deviation (RMSD), the slope of the best correlation line (slope), the correlation coefficient (R^2), and Kendall's rank correlation coefficient (τ_r) compared to experimental data. The latter was calculated only for the transformations that were explicitly studied, not for all combinations that can be formed from these transformations. Moreover, it was also evaluated considering only differences (both experimental and calculated) that are statistically significant at the 90% level ($\tau_{r,90}$).[41] Note that R^2 and the slope depend on the direction of the perturbation (i.e. whether $L_1 \rightarrow L_2$ or $L_2 \rightarrow L_1$ is considered, which is arbitrary). This was solved by considering both directions (both forward and backward, giving the same results but with the opposite sign) for all perturbations when these two measures were calculated. The standard deviation of the quality measures was obtained by a simple simulation approach.[42] For each transformation, 1000 Gaussian-distributed random numbers were generated with the mean and standard deviation equal to the MBAR and experimental results for that transformation. Then, the quality measures were then calculated for each of these 1000 sets of simulated results and the standard error over the 1000 sets is reported as the uncertainty. For fXa, no uncertainty for the experimental measurements was reported.[14] Therefore, we assumed a typical uncertainty of 2.4 (= 1.7 $\sqrt{2}$) kJ/mol for these values when estimating the precision of the quality measures.[43]

Result and Discussion

In this paper, we study whether it is possible to truncate periodic systems in FEP calculations, in the same way as we have done for spherical simulations.[11] We emphasize that the aim of this article is not to see whether the calculations reproduce the experimental affinities, but rather whether simulations of truncated systems reproduce the calculated results of the full (non-truncated) systems. We have studied two proteins and the results of these are described in separate sections.

DHFR results

We have studied the relative affinities of the seven nanomolar 2,4-diaminopyrimidine inhibitors of DHFR, shown in Figure 1.[15,16] The calculated affinities for the seven considered transformations are shown in Table 1. It can be seen that the precision of the calculated relative affinities is excellent, with standard errors of 0.02–0.12 kJ/mol, i.e. appreciably better than in the experiments (0.4–0.9 kJ/mol). Although it is not the primary aim of this article, it is satisfying to note that the calculations also reproduce the experimental relative affinities[16] well with errors of 0–3 kJ/mol, giving a MAD of only 1.6±0.2 kJ/mol and a R^2 of 0.79±0.04 (cf. Figure S1). Four of the transformations form a closed thermodynamic cycle (F→H→G→E→F), allowing us to estimate the convergence of the calculations. Quite satisfying, the cycle gives a free energy of 0.19±0.16 kJ/mol, showing that the simulations are converged within the estimated uncertainty.

The same seven ligands were also considered in our previous large-scale test of FEP calculations, but the simulations were performed on spherical systems and with only three λ values.[7] The results of those calculations are also included in Table 1. The old calculations gave a slightly worse precision with standard errors of 0.04–0.6 kJ/mol. In most cases, they underestimated the energy differences, probably owing to the too short simulations and integration errors caused by the low number of λ values. They reproduced the experimental results slightly worse, but for most quality measures, the difference is not statistically significant. In conclusion, the present calculations seem to be reliable and therefore can be used for calibration of the results obtained with truncated systems (for which the reproduction of experimental results is of a secondary interest).

Next, we truncated the protein by removing all residues with all atoms more than a certain distance r from the ligand (r = 25, 20, 15, and 10 Å were tested, retaining 207, 180, 137, and 78 of the 233 residues in the protein, respectively; cf. Table S1) and keeping atoms between r and r – 4 Å restrained in the MD simulations with a force constant of k_{res} = 4184 kJ/mol/Å^2. The relative binding energies for the seven transformations were then calculated from these simulations. The results in Figure 4a show that the truncation error (i.e. the difference in relative binding free energy of the truncated and full calculations) typically increases when the truncation radius is decreased: On average (last columns in Figure 4a), the truncation error varies between 1.1 and 3.6 kJ/mol as the truncation radius decreases from 25 to 10 Å. Clearly, a truncation radius of 10 Å is too small, giving a maximum error of 7 kJ/mol. However, already for a truncation radius of 25 Å, the maximum error is 3.8 kJ/mol. The precision of the truncated simulations is similar to that of the full simulations (0.02–0.12 kJ/mol for the various transformations, with a variation of only 0.01 kJ/mol between the various truncation radii; the raw data are shown in Table S1 in the supplementary material). Therefore, all truncation errors in Figure 4a are statistically significant at the 95%, except two (A→F and C→A at r = 25 Å). However, the cycle-closure hysteresis is somewhat larger for the truncated systems than for the full system, 0.4–1.0±0.2 kJ/mol, although it is not large enough to explain the truncation errors.

Consequently, the truncation errors are much larger than in our previous study of spherical systems.[11] To understand why periodic simulations are more sensitive to truncations than the spherical systems, we performed some additional test calculations. First, we recalculated the relative free energies without any periodicity (i.e. we wrapped all atoms in the snapshots of the periodic simulations into a single box, centred on the ligand and then recalculated the binding free energies from these snapshots without using any periodicity). The results in Figure 4b show that the errors are similar to those with the periodic systems (average errors of 1.0–3.7 kJ/mol and maximum errors of 2–8 kJ/mol). This indicates that periodicity is not the prime problem. We also made some calculations of the truncated systems in a water box with the same size as in the original system, showing errors of the same magnitude as with the smaller water boxes in Figure 4a. This also confirms that periodicity is not the problem.

Second, we tried to truncate the systems *after* the MD simulations, i.e. the snapshots of the full system were again wrapped into a single box, after which they were truncated, keeping the same

residues and the same number of water molecules (those closest to the ligand) as in the calculations leading to Figure 4a, and finally the free-energy differences were calculated without any periodicity. Figure 4c shows that the results of these calculations were totally different compared to when the truncation was performed before the MD simulations: The average truncation error was only 0.2–0.9 kJ/mol for all four truncation radii. In fact, only two transformation gave an error larger than 1 kJ/mol (both at r = 10 Å). This is quite amazing, considering that the truncated systems are quite strange, involving large volumes of empty space where protein residues were removed (note that this applies only to this truncation after MD and not to any of the other truncations in the article). However, the results clearly show that in energy terms, truncation of FEP calculations can be performed to quite small radii without any significant effect on the relative binding free energies. Unfortunately, there is no gain in computation time of truncating after the MD simulations, because the calculation of energies for the free-energy calculations are essentially for free, compared to the cost of running the simulation.

Consequently, we can conclude that the rather large truncation errors observed in Figure 4a are mainly caused by changes in the structures sampled in the MD simulations for the truncated systems. It may be that the truncated simulations allow too much movement of the atoms, compared to the full system. However, it is also possible that the restrained atoms in the simulations restrict the movement too much. We performed a set of test calculations for the E→G perturbation with different force constants for these restraint (cf. Table S2). These indicated that the restraints actually were too large. Therefore, we repeated the FEP calculations on the truncated systems with a force constant of only k_{res} = 1.3 kJ/mol/Å^2 (4184 kJ/mol/Å^2 in the previous calculations; calculations without any restraint gave similar results, but then some residues sometimes dissociated from the protein). From Figure 4d, it can be seen that the results are improved for all radii: The average error increases regularly from 0.6 kJ/mol at r = 25 Å to 3.0 kJ/mol at r = 10 Å, which are all smaller than the corresponding results in Figure 4a. The maximum errors are 1.9–5.1 kJ/mol. The precision (0.02–0.12 kJ/mol) is slightly lower in the simulations with the larger force constant.

The timing of the simulations of the truncated systems is shown in the last column of Table S1. It can be seen that r = 20 Å reduced the time consumption by a factor of two and that the smallest radius gave a reduction by a factor of four.

fXa simulations

To check that the results for DHFR are not specific for that protein, we have also considered another test case, viz. the binding of the ten 3-amidinobenzyl-1*H*-indole-2-carboxamide inhibitors in Figure 2 to blood-clotting factor Xa (fXa). The calculated affinities with the full protein are collected in Table 2. It can be seen that the calculated affinities reproduce experimental affinities[14] reasonably well, with errors for all transformations of 0–5 kJ/mol, except for the 63→39 transformation, for which the error is much larger, 10 kJ/mol. The present results are similar to those obtained for the same transformations with slightly different methods (periodic or spherical systems with 3–11 λ values),[7,10,11] with mean absolute differences of 1.4–2.8 kJ/mol. Thus, the previous calculations also had (even larger) problems with the 63→39 transformation. Therefore, the present calculations reproduce the experimental data slightly better than the previous calculations, with a MAD of 3.1±0.7 kJ/mol (3.9–4.5 kJ/mol for the previous studies; Figure S2). The standard errors of the affinity estimates are 0.3–0.8 kJ/mol. This is similar to the previous calculations with periodic systems,[10] but larger than the calculations with spherical systems and 11 λ values (0.1–0.3 kJ/mol).[11] Again, the new calculations seem reliable and can therefore be used as a reference for the truncated calculations.

Next, we truncated the protein in the same way as for DHFR, testing r = 35, 30, 25, 20, 15, and 10 Å (more radii than for DHFR because the protein is larger). This corresponds to 280–83 of the 288 residues in the protein, as can be seen in Table S3. The results for these calculations are shown

in Figure 5a, presented as the difference compared to the full-protein calculation (raw data are given in Table S3).

It can be seen that for r = 35 Å, all results agree with those using the full system within 0.6 kJ/mol (0.3 kJ/mol on average). However, already for r = 30 Å, the maximum error has increased to 1.8 kJ/mol (0.9 kJ/mol on average). For r = 25 Å, the truncation error for the problematic 63→39 transformation is 3.6 kJ/mol, whereas it is up to 1.9 kJ/mol for the other transformations and the average error is 1.1 kJ/mol. However, for smaller radii, the truncation error for the other transformations also start to increase, with maximum errors of 5.1–5.6 kJ/mol. The average errors are 2.1, 2.3, and 2.5 kJ/mol for r = 20, 15, and 10 Å, respectively.

The standard error remains within 0.1 kJ/mol of that for the full simulations for all transformations. Consequently, for r = 35 Å, none of the differences between the full and truncated simulations is statistically significant (at 95% confidence). However, already at r = 30 Å two of the differences are statistically significant and this increases to six of the eight transformations at r = 10 Å.

The timing of the various truncated calculations is shown in Table S3. It can be seen that r = 25 Å gave reduction of the time consumption by a factor of two and the smallest radius gave a reduction by almost a factor of 4.

To see whether the results improved also for fXa if the restraints are reduced, we repeated the simulations for the truncated systems with the force constant for the restrained atoms reduced to k_{res} = 1.3 kJ/mol/Å^2. From Figure 5b, it can be seen that the results are clearly improved for the smaller truncation radii: For r = 10 Å, the maximum truncation error is reduced from 5.6 to 3.1 kJ/mol (average error from 2.5 to 1.5 kJ/mol). Similar improvements are observed also for r = 15 and 20 Å, and also for the maximum error at r = 25 Å, although the average errors are the same (1.1 kJ/mol). However, for the two largest radii, the maximum error is actually slightly larger with the smaller force constant (e.g. 1.3 kJ/mol compared to 0.6 kJ/mol for r = 35 Å). This reflects that the results with the smaller force constant are somewhat more uneven with less clear trends. On the other hand, the precision of the two sets of simulations is identical (0.2–0.6 kJ/mol).

Conclusions

In this article, we have studied whether FEP calculations of ligand-binding affinities can be sped up by truncating the simulated protein in calculations involving periodic systems treated with particle-mesh Ewald summation. We have employed two different proteins, DHFR and fXa to study how the truncation effects depend on the simulated systems. The results are qualitatively similar, indicating that they are probably quite general. For both systems, the average truncation error increases as the truncation radius is decreased. Keeping atoms between r and r – 4 Å restrained towards the starting structure with a large force constant gives large truncation errors, especially for small radii, e.g. with maximum errors of 6–7 kJ/mol and average errors of 2.5–3.6 kJ/mol for r = 10 Å. The errors do not seem to be caused by the enforced periodicity, but rather by the change in the sampled structures, partly owing to the strong restraints on the outer atoms. In fact, the results can be improved by reducing the force constant of the restraints to k_{res} = 1.3 kJ/mol/Å^2. Then, the maximum and average error at r = 10 Å are reduced to 3–5 and 1.5–3.0 kJ/mol, respectively.

However, the truncation errors are still quite sizeable: Only for four systems, with $r \geq 20$ Å, are the average error below 1 kJ/mol. In particular, the errors are appreciably larger than for the spherical systems, studied in our previous investigation using the Q software.[12] In those calculations, the simulated system for fXa could be reduced from around 39 000 to 1500 atoms without affecting the calculated affinities by more than 0.5 kJ/mol on average (maximum change 1.4 kJ/mol). The reason for this is partly technical: With the Q software, the whole protein was included in the calculations, but the outer parts (outside the truncation) was kept fixed and those atoms did not contribute to the time-consuming calculations. Still they prohibit any non-physical

movement of the remaining atoms and avoids that water molecules occupy space that that is part of the protein. However, in Amber, also fixed atoms contribute fully to the time-consumption and all simulated atoms must fit into the simulated periodic box, with a significant buffer of water molecules. Therefore, residues must be removed in the Amber calculations (entire residues to keep an integer net charge) and a buffer of restrained atoms needs to be included to avoid unphysical movements of the remaining residues, especially those that are no longer covalently connected (if the restraint is removed, some residues dissociate from the protein). Finally, in the spherical calculations, atoms were removed based on a radius from a single central atom in the ligand (the nitrogen atom of the indole ring, cf. Figure 2), whereas in the present calculations, residues with any atom within a certain distance from any atom in the ligand were included in the calculations. Therefore, for the same truncation radius, the present calculations contain many more atoms than in the spherical calculations.

Consequently, it seems to be much harder to truncate periodic simulations than spherical simulations. In fact, the timings show that for the smallest radius (r = 10 Å), the time consumption is reduced only by a factor of four. Thus, such a simulation takes approximately the same time as the corresponding Q simulation with the most truncated system. Considering that the truncation errors were smaller with the spherical simulations, we have to conclude that there does not seem to be any gain of truncating periodic simulations.

It can be noted that our results are in accordance with conclusions obtained from the related problem of truncating the electrostatic interactions in MD simulations:[44] Simulations with cut-offs smaller than 15 Å are not recommended because they give rise to severe artefacts in the simulations, in particular for inhomogeneous systems and at interfaces between regions of high and low dielectric constants. Moreover, truncation will of course not give accurate results if the binding of ligands gives rise to changes in the conformation of the protein outside the truncated region that is different for different ligands and significantly affects the binding.

Still, the results in Figure 4c are promising, showing that if the truncation is made *after* the MD simulation (i.e. if the MM free energies are calculated for truncated snapshots without periodicity from the original MD simulation), the average truncation error is less than 0.9 kJ/mol for all tested radii (maximum error less than 1.4 kJ/mol). At first thought, this may not seem very impressive, because the time consumption is completely dominated by the MD simulations. However, the results show that post-processing of FEP results can be performed with much smaller systems than those simulated by MD. This would be of great interest if the post-processing is performed with a more expensive energy function, e.g. a polarisable force field or with quantum-mechanical methods. However, it should be noted that such free energies are strictly not valid, because they are based on structures sampled with one method and energies calculated with another method.[45] Still, many widely used approaches ignore this problem, e.g. the MM/GBSA approach for ligand binding, for which structures are sampled by MD in explicit solvent, whereas energies are calculated with a continuum-solvation method.[46,47]

Acknowledgements

This investigation has been supported by grants from the Swedish research council (project 2014-5540), from Knut and Alice Wallenberg Foundation (KAW 2013.0022), and from the European Spallation Source consortium. The computations were performed on computer resources provided by the Swedish National Infrastructure for Computing (SNIC) on Lunarc at Lund University and HPC2N at Umeå University.

Supporting Information

Raw data of the truncated simulations for DHFR and fXa, test of different force constants, and comparison of calculated and experimental results.

References

(1) Gohlke, H.; Klebe, G. Approaches to the Description and Prediction of the Binding Affinity of Small-Molecule Ligands to Macromolecular Receptors. *Angew. Chemie - Int. Ed.* **2002**, *41* (15), 2644–2676.

(2) Hansen, N.; Van Gunsteren, W. F. Practical Aspects of Free-Energy Calculations: {A} Review. *J. Chem. Theory Comput.* **2014**, *10* (7), 2632–2647.

(3) Mobley, D. L.; Klimovich, P. V. Perspective: Alchemical Free Energy Calculations for Drug Discovery. *J. Chem. Phys.* **2012**, *137*, 230901.

(4) Michel, J.; Essex, J. W. Prediction of Protein-Ligand Binding Affinity by Free Energy Simulations: Assumptions, Pitfalls and Expectations. *J. Comput. Aided. Mol. Des.* **2010**, *24* (8), 639–658.

(5) Jorgensen, W. L. Effcient Drug Lead Discovery and Optimization. *Acc. Chem. Res.* **2009**, *42* (6), 724–733.

(6) Christ, C.; Fox, T. Accuracy Assessment and Automation of Free Energy Calculations for Drug Design. *J. Chem. Inf. Model.* **2013**, *54*, 108–120.

(7) Mikulskis, P.; Genheden, S.; Ryde, U. A Large-Scale Test of Free-Energy Simulation Estimates of Protein-Ligand Binding Affinities. *J. Chem. Inf. Model.* **2014**, *54* (10), 2794–2806.

(8) Wang, L.; Wu, Y.; Deng, Y.; Kim, B.; Pierce, L.; Krilov, G.; Lupyan, D.; Robinson, S.; Dahlgren, M. K.; Greenwood, J.; Romero, D. L.; Masse, C.; Knight, J. L.; Steinbrecher, T.; Beuming, T.; Damm, W.; Harder, E.; Sherman, W.; Brewer, M.; Wester, R.; Murcko, M.; Frye, L.; Farid, R.; Lin, T.; Mobley, D. L.; Jorgensen, W. L.; Berne, B. J.; Friesner, R. A.; Abel, R. Accurate and Reliable Prediction of Relative Ligand Binding Potency in Prospective Drug Discovery by Way of a Modern Free-Energy Calculation Protocol and Force Field. *J. Am. Chem. Soc.* **2015**, *137* (7), 2695–2703.

(9) Harder, E.; Damm, W.; Maple, J.; Wu, C.; Reboul, M.; Xiang, J. Y.; Wang, L.; Lupyan, D.; Dahlgren, M. K.; Knight, J. L.; Kaus, J. W.; Cerutti, D. S.; Krilov, G.; Jorgensen, W. L.; Abel, R.; Friesner, R. A. OPLS3: A Force Field Providing Broad Coverage of Drug-like Small Molecules and Proteins. *J. Chem. Theory Comput.* **2016**, *12*, 281–296.

(10) Genheden, S.; Nilsson, I.; Ryde, U. Binding Affinities of Factor Xa Inhibitors Estimated by Rigorous and Simplified Methods. *J. Chem. Inf. Model.* **2010**, *51*, 947–958.

(11) Genheden, S.; Ryde, U. Improving the Efficiency of Protein-Ligand Binding Free-Energy Calculations by System Truncation. *J. Chem. Theory Comput.* **2012**, *8* (4), 1449–1458.

(12) Marelius, J.; Kolmodin, K.; Feierberg, I.; Åqvist, J. Q: An MD Program for Free Energy Calculations and Empirical Valence Bond Simulations in Biomolecular Systems. *J. Mol. Graph. Model.* **1999**, *16*, 213–225.

(13) Darden, T.; York, D.; Pedersen, L. Particle Mesh Ewald: An N -log(N) Method for Ewald Sums in Large Systems. *J. Chem. Phys.* **1993**, *98*, 10089–10092.

(14) Matter, H.; Defossa, E.; Heinelt, U.; Blohm, P.-M.; Schneider, D.; Müller, A.; Herok, S.; Schreuder, H.; Liesum, A.; Brachvogel, V.; Lönze, P.; Walser, A.; Al-Obeidi, F.; Wildgoose, P. Design and Quantitative Structure-Activity Relationship of 3-Amidinobenzyl-1 H -Indole-2-Carboxamides as Potent, Nonchiral, and Selective Inhibitors of Blood Coagulation Factor Xa. *J. Med. Chem.* **2002**, *45*, 2749–2769.

(15) Yuthavong, Y.; Vilaivan, T.; Chareonsethakul, N.; Kamchonwongpaisan, S.; Sirawaraporn, W.; Quarrell, R.; Lowe, G. Development of a Lead Inhibitor for the A16V+S108T Mutant of Dihydrofolate Reductase from the Cycloguanil-Resistant Strain (T9/94) of Plasmodium

Falciparum. *J. Med. Chem.* **2000**, *43*, 2738–2744.
(16) Tarnchompoo, B.; Sirichaiwat, C.; Phupong, W.; Intaraudom, C.; Sirawaraporn, W.; Kamchonwongpaisan, S.; Vanichtanankul, J.; Thebtaranonth, Y.; Yuthavong, Y. Development of 2,4-Diaminopyrimidines as Antimalarials Based on Inhibition of the S108N and C59R+S108N Mutants of Dihydrofolate Reductase from Pyrimethamine-Resistant Plasmodium Falciparum. *J. Med. Chem.* **2002**, 1244–1252.
(17) Rastelli, G.; del rio, A.; Degliesposti, G.; Sgobba, M. Fast and Accurate Predictions of Binding Free Energies Using MM-PBSA and MM-GBSA. *J. Comput. Chem.* **2010**, *31*, 797–810.
(18) Yuvaniyama, J.; Chitnumsub, P.; Kamchonwongpaisan, S.; Vanichtanankul, J.; Sirawaraporn, W.; Taylor, P.; Walkinshaw, M. D.; Yuthavong, Y. Insights into Antifolate Resistance from Malarial DHFR-TS Structures. *Nat. Struct. Biol.* **2003**, *10*, 357–365.
(19) Kongsted, J.; Ryde, U. An Improved Method to Predict the Entropy Term with the MM/PBSA Approach. *J. Comput. Aided. Mol. Des.* **2009**, *23* (2), 63–71.
(20) Hornak, V.; Abel, R.; Okur, A.; Strockbine, B.; Roitberg, A.; Simmerling, C. Comparison of Multiple Amber Force Fields and Development of Improved Protein Backbone Parameters. *Proteins Struct. Funct. Bioinforma.* **2006**, *65*, 712–725.
(21) Cornell, W. D.; Cieplak, P.; Bayly, C. I.; Gould, I. R.; Merz, K. M.; Ferguson, D. M.; Spellmeyer, D. C.; Fox, T.; Caldwell, J. W.; Kollman, P. A. A Second Generation Force Field for the Simulation of Proteins, Nucleic Acids, and Organic Molecules. *J. Am. Chem. Soc.* **1995**, *117* (19), 5179–5197.
(22) Wang, J. M.; Wolf, R. M.; Caldwell, J. W.; Kollman, P. A.; Case, D. A. Development and Testing of a General Amber Force Field. *J. Comput. Chem.* **2004**, *25* (9), 1157–1174.
(23) Bayly, C. I.; Cieplak, P.; Cornell, W. D.; Kollman, P. A. A Well-Behaved Electrostatic Potential Based Method Using Charge Restraints for Deriving Atomic Charges: The RESP Model. *J. Phys. Chem.* **1993**, *97*, 10269–10280.
(24) Besler, B. H.; Merz, K. M.; Kollman, P. A. Atomic Charges Derived from Semiempirical Methods. *J. Comput. Chem.* **1990**, *11* (4), 431–439.
(25) Jorgensen, W. L.; Chandrasekhar, J.; Madura, J. D.; Impey, R. W.; Klein, M. L. Comparison of Simple Potential Functions for Simulating Liquid Water. *J. Chem. Phys.* **1983**, *79* (2), 926–935.
(26) Case, D. A.; Darden, T. A.; Cheatham, III, T. E.; Simmerling, C. L.; Wang, J.; Duke, R. E.; Luo, R.; Walker, R. C.; Zhang, W.; Merz, K. M.; Roberts, B.; Wang, B.; Hayik, S.; Roitberg, A.; Seabra, G.; Kolossváry, I.; Wong, K. F.; Paesani, F.; Vanicek, J.; Wu, X.;, A.; P.A., K. Amber 11. University of California, San Francisco 2010.
(27) Case, D. A.; Darden, T. A.; Cheatham, III, T. E.; Simmerling, C. L.; Wang, J.; Duke, R. E.; Luo, R.; Walker, R. C.; Zhang, W.; Merz, K. M.; Roberts, B.; Wang, B.; Hayik, S.; Roitberg, A.; Seabra, G.; Swails, J.; Götz, A. W.; Kolossváry, I.; Wong, K. F.; Paesani, F.; Vanicek, J.; Wolf, R. M.; Liu, J.; Wu, X.; Brozell, S. R.; Steinbrecher, T.; Gohlke, H.; Cai, Q.; Ye, X.; Wang, J.; Hsieh, M.-J.; Cui, G.; Roe, D. R.; Mathews, D. H.; Seetin, M. G.; Salomon-Ferrer, R.; Sagui, C.; Babin, V.; Luchko, T.; Gusarov, S.; Kovalenko, A.; Kollman, P. A. Amber 12. University of California, San Francisco 2012.
(28) Wu, X.; Brooks, B. R. Self-Guided Langevin Dynamics Simulation Method. *Chem. Phys. Lett.* **2003**, *381* (3–4), 512–518.
(29) Berendsen, H. J. C.; Postma, J. P. M.; van Gunsteren, W. F.; DiNola, A.; Haak, J. R. Molecular Dynamics with Coupling to an External Bath. *J. Chem. Phys.* **1984**, *81* (June), 3684–3690.
(30) Ryckaert, J. P.; Ciccotti, G.; Berendsen, H. J. C. Numerical Integration of the Cartesian Equations of Motion of a System with Constraints: Molecular Dynamics of N-Alkanes. *J. Comput. Phys.* **1977**, *23* (3), 327–341.

(31) Yang, W.; Bitetti-Putzer, R.; Karplus, M. Free Energy Simulations: Use of Reverse Cumulative Averaging to Determine the Equilibrated Region and the Time Required for Convergence. *J. Chem. Phys.* **2004**, *120* (6), 2618–2628.
(32) Gilson, M. K.; Given, J. A.; Bush, B. L.; Mccammon, J. A. The Statistical-Thermodynamic Basis for Computation of Binding Affinities : A Critical Review. **1997**, *72*, 1047–1069.
(33) Shirts, M. R.; Chodera, J. D. Statistically Optimal Analysis of Samples from Multiple Equilibrium States. *J. Chem. Phys.* **2008**, *129* (124105).
(34) Bennett, C. H. MC Method for FEP. Argues That It Is Always Better to Sample Both Ensembles than Only One. Discusses Overlap and Efficiency. *J. Comput. Phys.* **1976**, *22*, 245–268.
(35) Zwanzig, R. W. High-Temperature Equation of State by a Perturbation Method. I. Nonpolar Gases. *J. Chem. Phys.* **1954**, *22* (8), 1420–1426.
(36) Kirkwood, J. G. Statistical Mechanics of Fluid Mixtures. *J. Chem. Phys.* **1935**, *3* (5), 300.
(37) Steinbrecher, T.; Mobley, D. L.; Case, D. A. Nonlinear Scaling Schemes for Lennard-Jones Interactions in Free Energy Calculations. *J. Chem. Phys.* **2007**, *127* (21), 1–13.
(38) Steinbrecher, T.; Joung, I.; Case, D. A. Soft-Core Potentials in Thermodynamic Integration: Comparing One-and Two-Step Transformations. *J. Comput. Chem.* **2011**, *32* (15), 3253–3263.
(39) Case, D. A.; Cerutti, T. E.; Cheatham, III, T. E.; Darden, T. A.; Duke, R. E.; Giese, T. J.; Gohlke, H.; Goetz, A. W.; Greene, D.; Homeyer, N.; Izadi, S.; Kovalenko, A.; Lee, T. S.; LeGrand, S.; Li, P.; Lin, C.; Liu, J.; Luchko, T.; Luo, R.; Mermelstein, D.; Merz, K. M.; Monard, G.; Nguyen, H.; Omelyan, I. P.; Onufriev, A. V.; Pan, F.; Qi, R.; Roe, D. R.; Roitberg, A. E.; Sagui, C.; Simmerling, C. L.; Botello-Smith, W. M.; Swails, J.; Walker, R. C.; Wang, J.; Wolf, R. M.; Wu, X.; Xiao, L.; York, D. M.; Kollman, P. A. Amber 16. University of California, San Francisco 2017.
(40) Kaus, J. W.; Pierce, L. T.; Walker, R. C.; McCammon, J. A. Improving the Efficiency of Free Energy Calculations in the Amber Molecular Dynamics Package. *J. Chem. Theory Comput.* **2013**, *9*, 4131–4139.
(41) Mikulskis, P.; Genheden, S.; Rydberg, P.; Sandberg, L.; Olsen, L.; Ryde, U. Binding Affinities in the SAMPL3 Trypsin and Host-Guest Blind Tests Estimated with the MM/PBSA and LIE Methods. *J. Comput. Aided. Mol. Des.* **2012**, *26* (5), 527–541.
(42) Genheden, S.; Ryde, U. How to Obtain Statistically Converged MM/GBSA Results. *J. Comput. Chem.* **2010**, *31* (4), 837–846.
(43) Brown, S. P.; Muchmore, S. W.; Hajduk, P. J. Healthy Skepticism: Assessing Realistic Model Performance. *Drug Discov. Today* **2009**, *14* (7–8), 420–427.
(44) Cisneros, G. A.; Karttunen, M.; Ren, P. Y.; Sagui, C. Classical Electrostatics for Biomolecular Simulations (Vol 114, Pg 779, 2014). *Chem. Rev.* **2014**, *114*, 779–814.
(45) Ryde, U.; Söderhjelm, P. Ligand-Binding Affinity Estimates Supported by Quantum-Mechanical Methods. *Chem. Rev.* **2016**, *116*, 5520–5566.
(46) Genheden, S.; Ryde, U. The MM/PBSA and MM/GBSA Methods to Estimate Ligand-Binding Affinities. *Expert Opin. Drug Discov.* **2015**, *441*, 1–13.
(47) Godschalk, F.; Genheden, S.; Söderhjelm, P.; Ryde, U. Comparison of MM/GBSA Calculations Based on Explicit and Implicit Solvent Simulations. *Phys. Chem. Chem. Phys.* **2013**, *15* (20), 7731–7739.

Table 1. Results for the FEP calculations on DHFR with the full enzyme (kJ/mol). Experimental results[16] and results from our previous calculations with a spherical system and only three λ values[7] are also included. Note that two of the transformations were studied in the opposite direction in that study. In the second part of the table, quality measures for the calculated data are given: the mean absolute deviation (MAD) from experimental results, root-mean-squared deviation (RMSD), the slope of the best correlation line, the correlation coefficient (r^2), Kendall's rank-correlation coefficient, based only on the calculated transformations (τ_r), and the same coefficient evaluated only for differences that are statistically significant at the 90% level ($\tau_{r,90}$).

	periodic, 13 λ	spherical, 3 λ[7]	Exp.[16]
A→F	1.76±0.12	2.7±0.6	3.0±0.9
B→A	0.02±0.02	-0.1±0.04	1.7±0.9
C→A	-0.71±0.04	-0.1±0.1	1.0±0.9
E→G	7.71±0.05	2.9±0.2	7.1±0.4
F→E	0.65±0.10	2.9±0.6	0.5±0.4
F→H	7.62±0.06	2.8±0.2	4.2±0.4
H→G	0.93±0.10		3.4±0.4
MAD	1.6±0.2	1.9±0.3	
RMSD	1.9±0.2	2.3±0.2	
slope	1.02±0.05	0.51±0.03	
R^2	0.79±0.04	0.66±0.06	
τ_r	0.71±0.11	0.33±0.20	
$\tau_{r,90}$	1.00±0.02	1.00±0.02	

Table 2. Experimental[14] and calculated relative binding affinities for fXa (kJ/mol) with the full protein. Results from our three previous investigations were also included.[7,10,11] The second part of the table lists the same quality measures as in Table 1.

	Exp.[14]	periodic, 11 λ	spherical, 3 λ[7]	spherical, 11 λ[11]	periodic, 9 λ[10]
5→47	-4.9	-2.4±0.8	0.5±0.5	0.2±0.3	
53→9	-1.9	-1.7±0.5	-0.4±0.3	-0.6±0.1	-1.2±0.5
53→47	-2.5	-0.7±0.4	-1.6±0.6	-1.1±0.2	-1.1±0.5
53→49	2.5	-0.2±0.5	1.2±0.2	-1.1±0.1	-1.8±0.6
53→50	-1.9	-0.9±0.6	0.8±0.2	-0.4±0.1	-0.2±0.7
53→51	3.5	-1.8±0.6	0.5±0.2	-0.6±0.1	
125→53	-1.0	-2.1±0.3	-0.3±0.1	-0.2±0.1	-2.4±0.4
63→39	10.1	0.0±0.6	-10.3±0.7	-3.8±0.2	-4.0±0.8
MAD		3.1±0.7	4.5±0.7	3.9±0.7	3.9±0.8
RMSD		4.3±0.8	7.6±0.9	5.6±0.8	6.1±1.1
slope		0.1±0.1	-0.6±0.1	-0.2±0.04	-0.3±0.1
R^2		0.06±0.07	-0.54±0.12	-0.53±0.12	-0.41±0.14
τ_r		0.25±0.28	0.25±0.27	0.00±0.26	0.33±0.32
$\tau_{r,90}$		1.00±0.29	-1.00±0.00	-1.00±0.00	-1.00±0.00

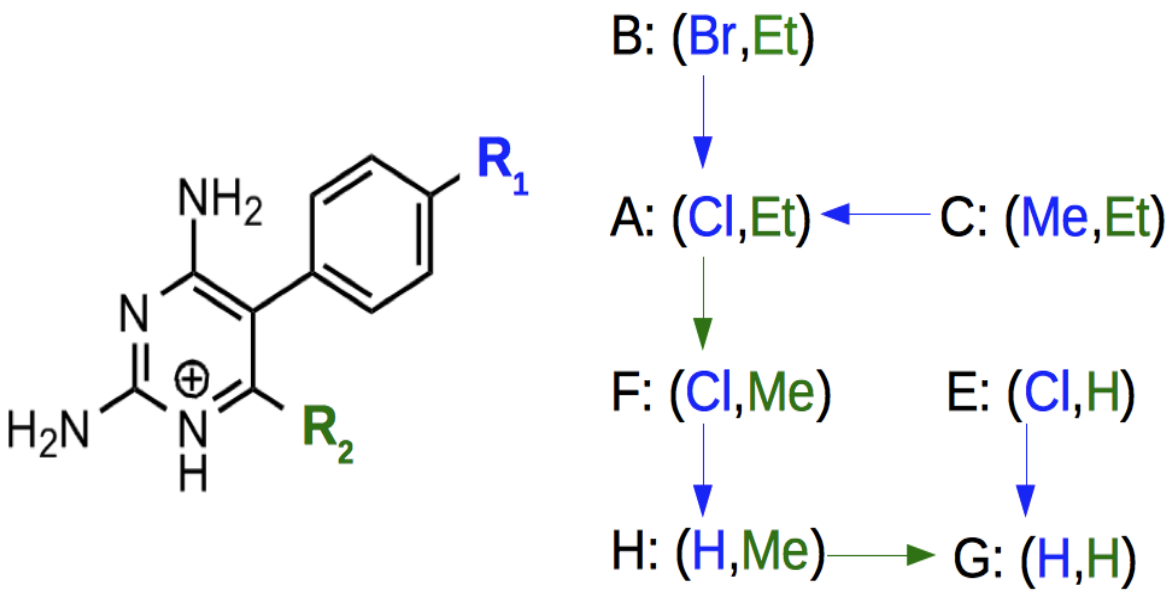

Figure 1. The seven DHFR ligands considered and the six studied transformations.

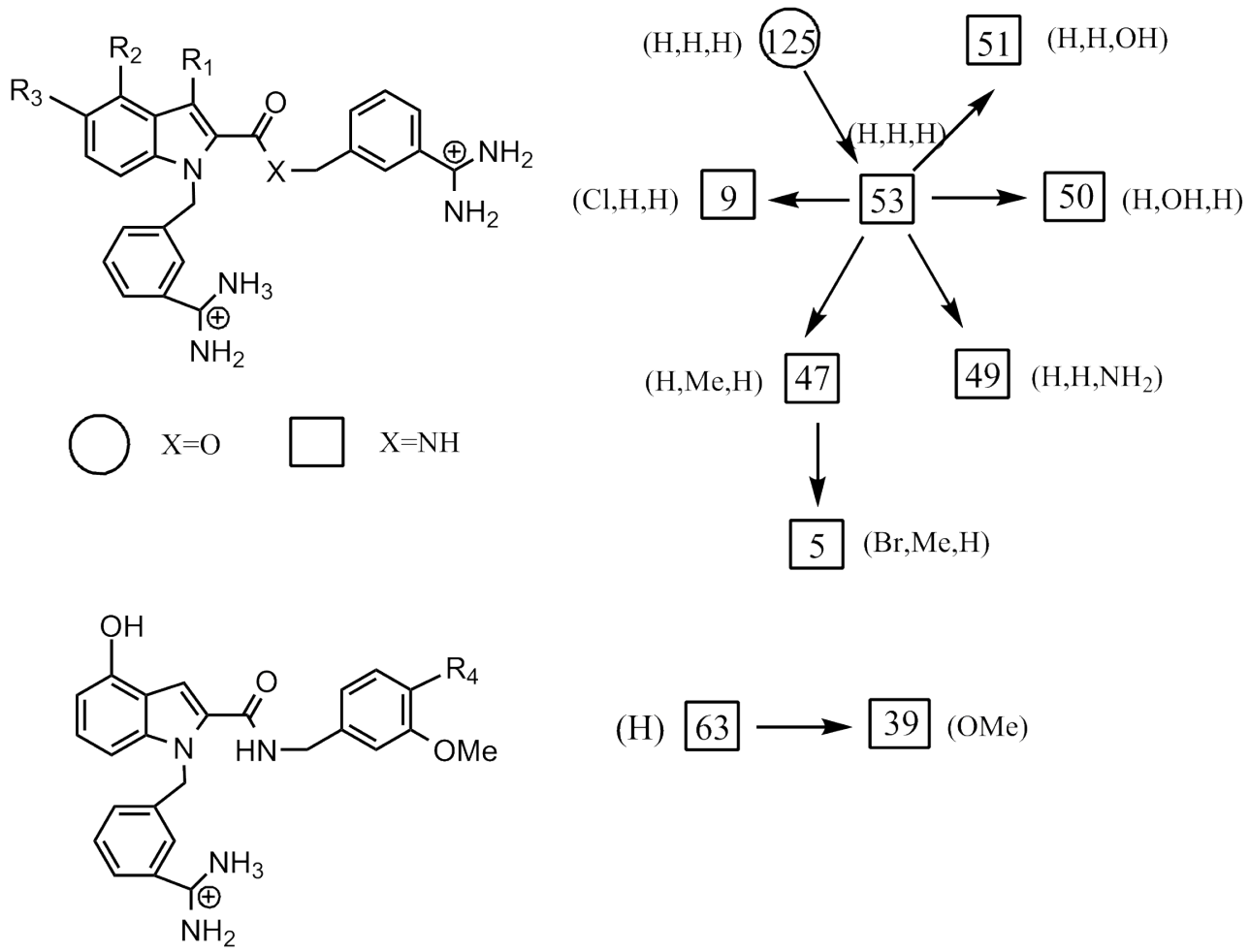

Figure 2. Factor Xa ligands and transformations considered in this study. The three groups in brackets in the upper right part of the figure are the R_1, R_2, R_3 groups, whereas the single group in the lower right part is the R_4 group.

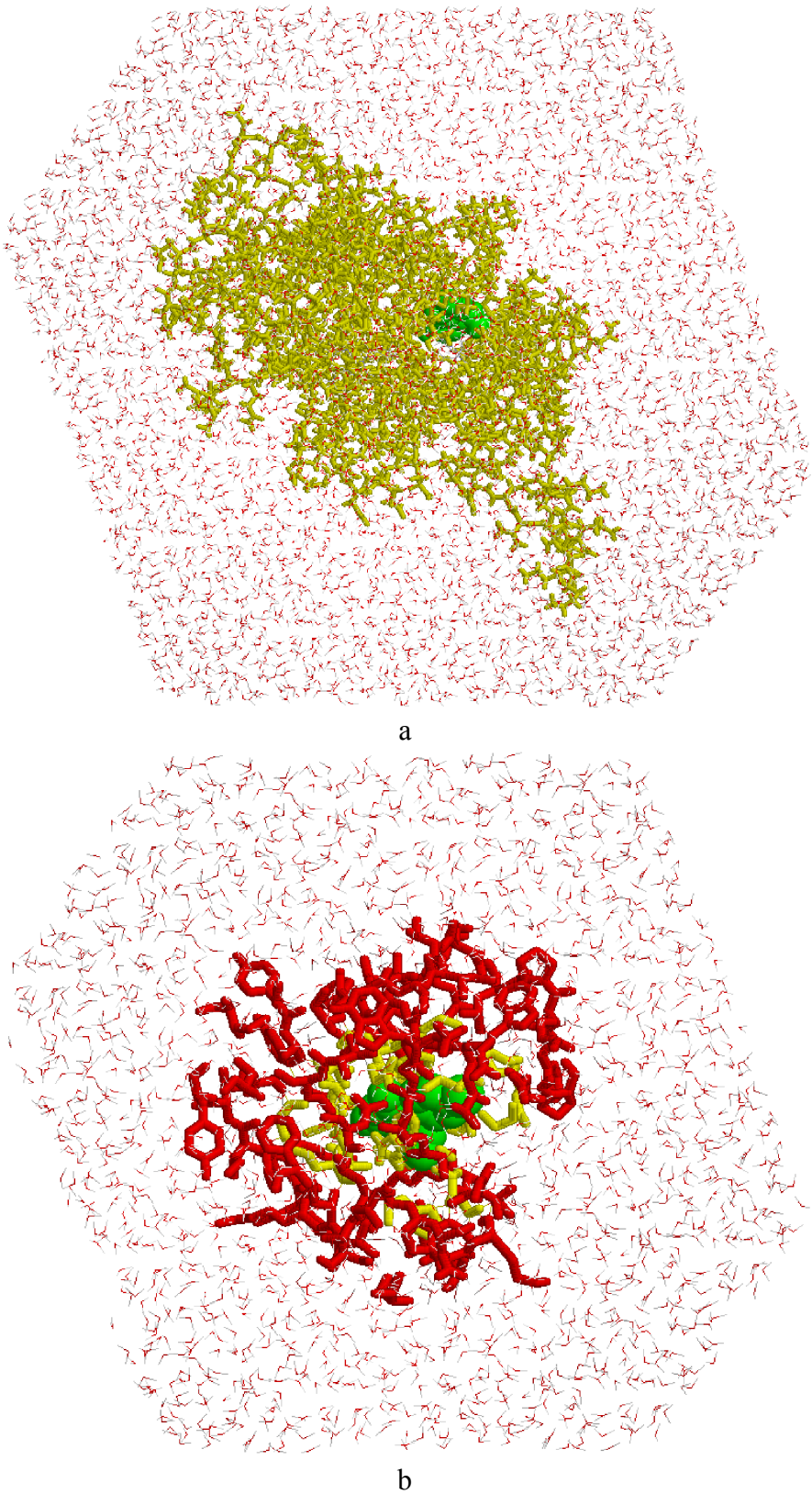

Figure 3. DHFR before (a) and after (b) the r = 10 Å truncation. The ligand is shown in green space filling, the protein in yellow sticks and water molecules in wireframe. In (b) restrained atoms are shown in red.

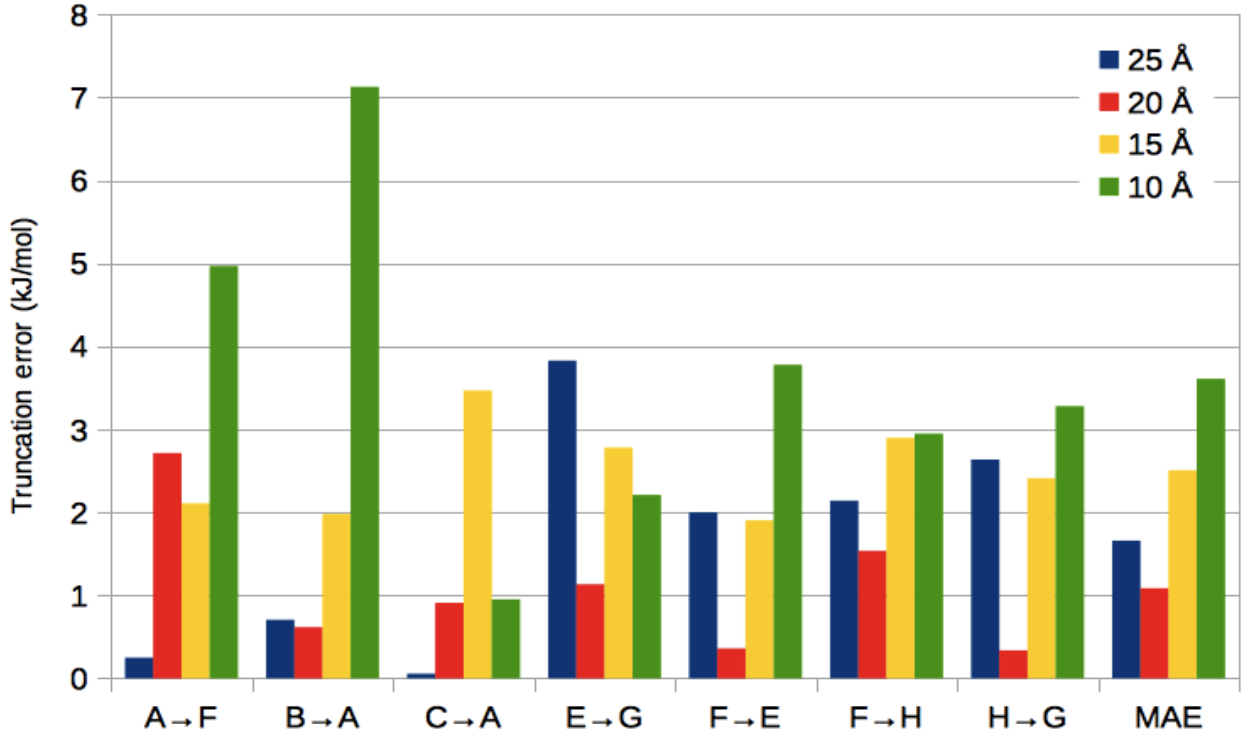
Truncation error (kJ/mol)
0
1
2
3
4
5
6
7
8
25 Å
20 Å
15 Å
10 Å
A→F
B→A
C→A
E→G
F→E
F→H
H→G
MAE

a

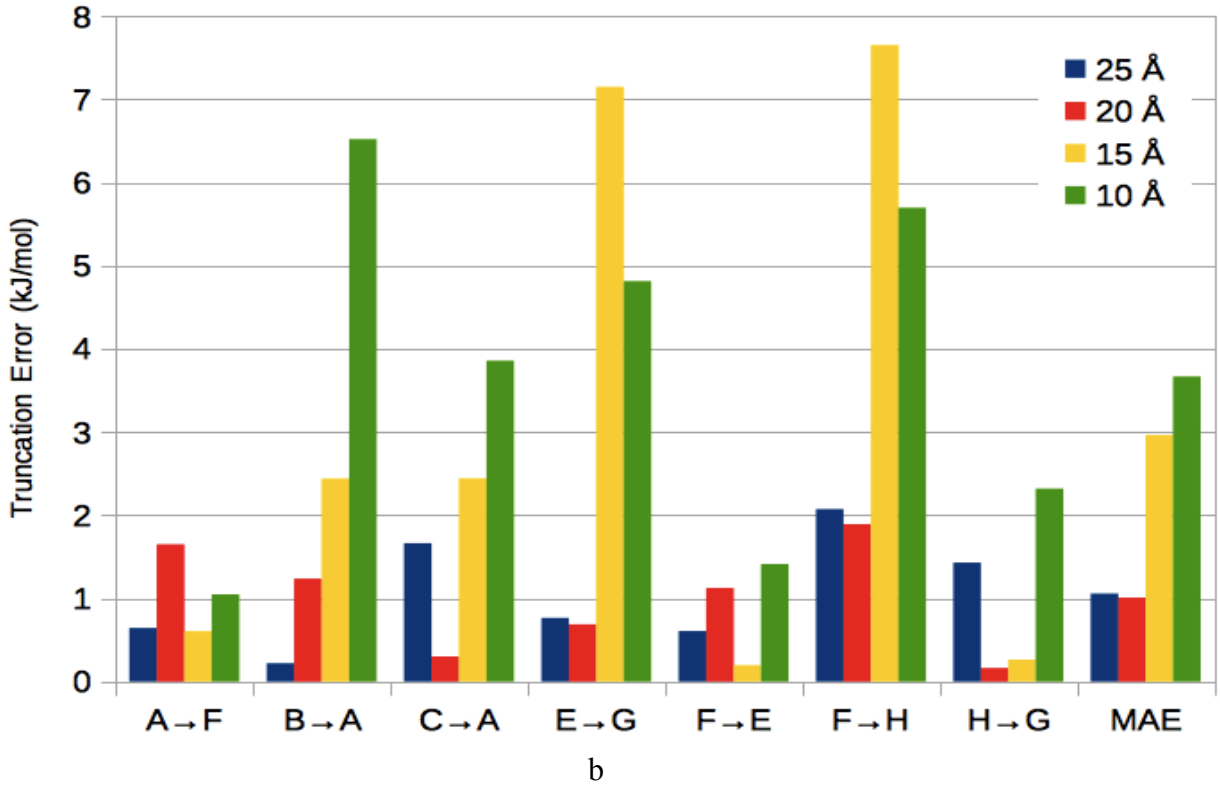
Truncation Error (kJ/mol)
0
1
2
3
4
5
6
7
8
25 Å
20 Å
15 Å
10 Å
A→F
B→A
C→A
E→G
F→E
F→H
H→G
MAE

b

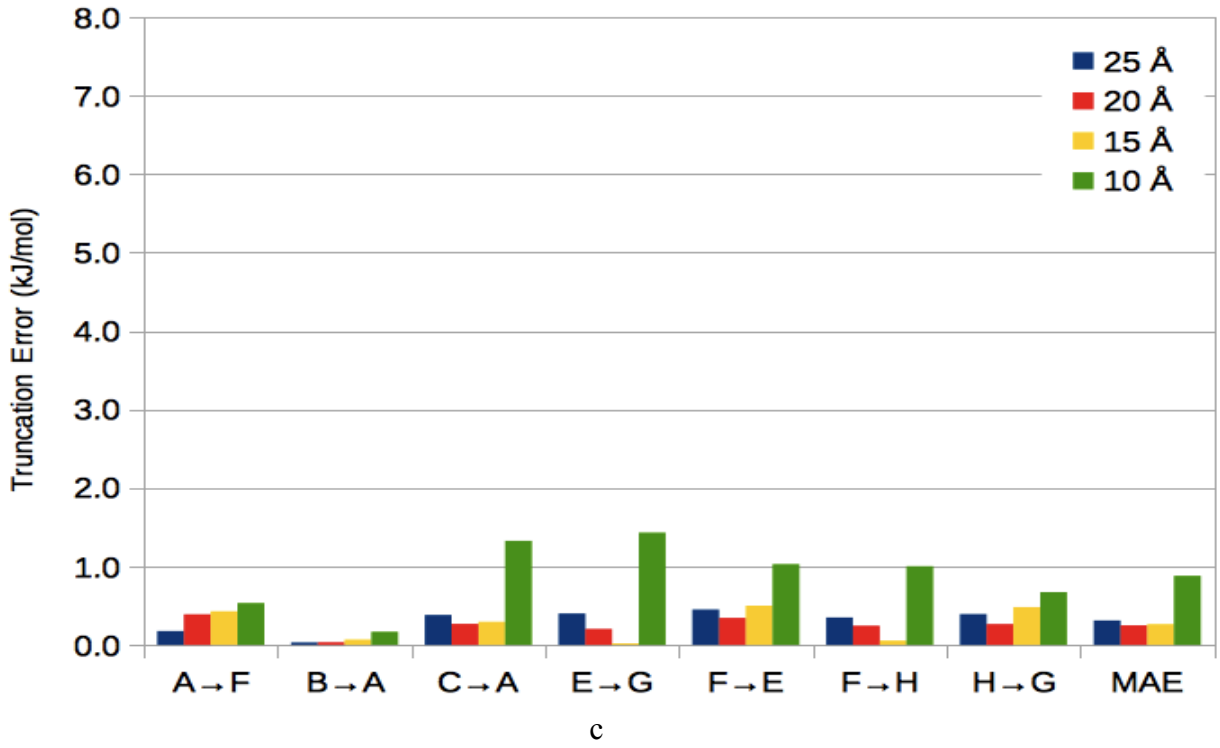

c

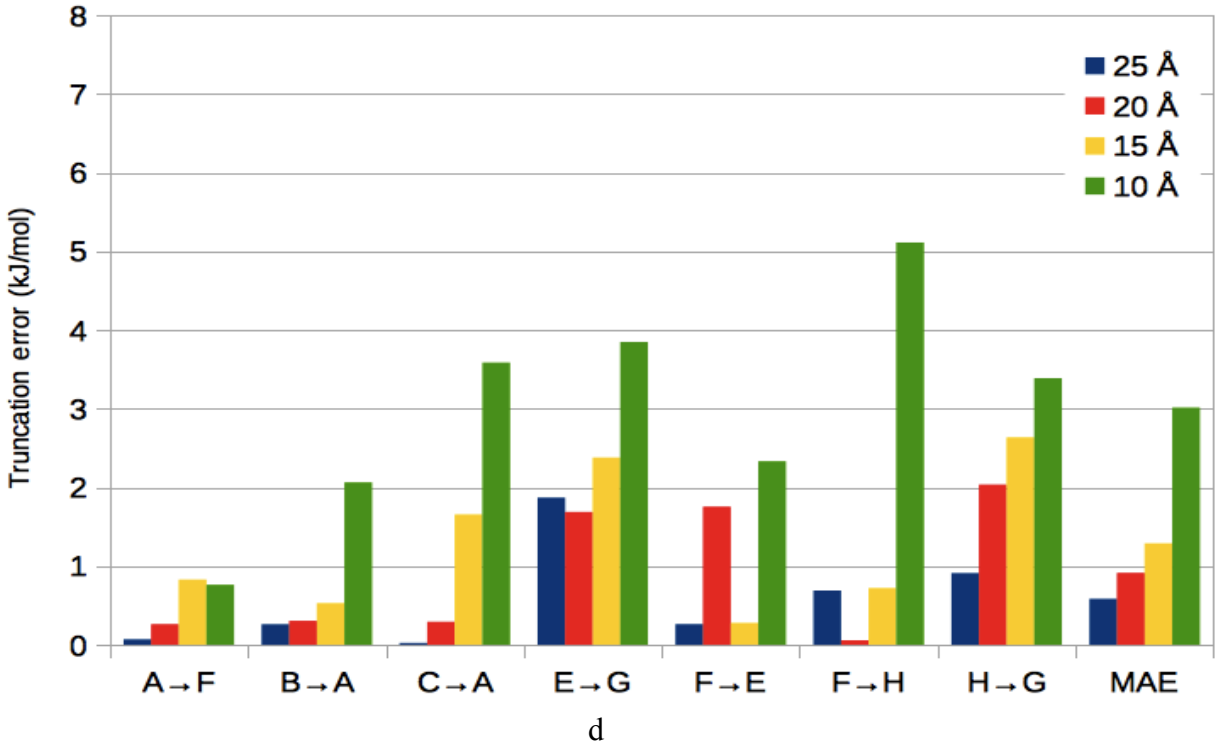

d

Figure 4. Effect of the truncations of the FEP calculations for DHFR. The results are presented as the absolute difference between the full and the truncated simulation for each of the six studied transformations for DHFR. The last column shows the mean absolute error (MAE) over the six transformations. (a) Standard calculations with atoms within r and r – 4 Å restrained towards the crystal structure with a force constant of k_{res} = 4184 kJ/mol/Å^2. (b) The same calculations, but with free energies calculated without periodicity. (c) The same calculations, but truncated after the MD and calculated without periodicity. (d) Calculations performed with k_{res} = 1.3 kJ/mol/Å^2. The uncertainties in the truncation errors are 0.03–0.17 kJ/mol.

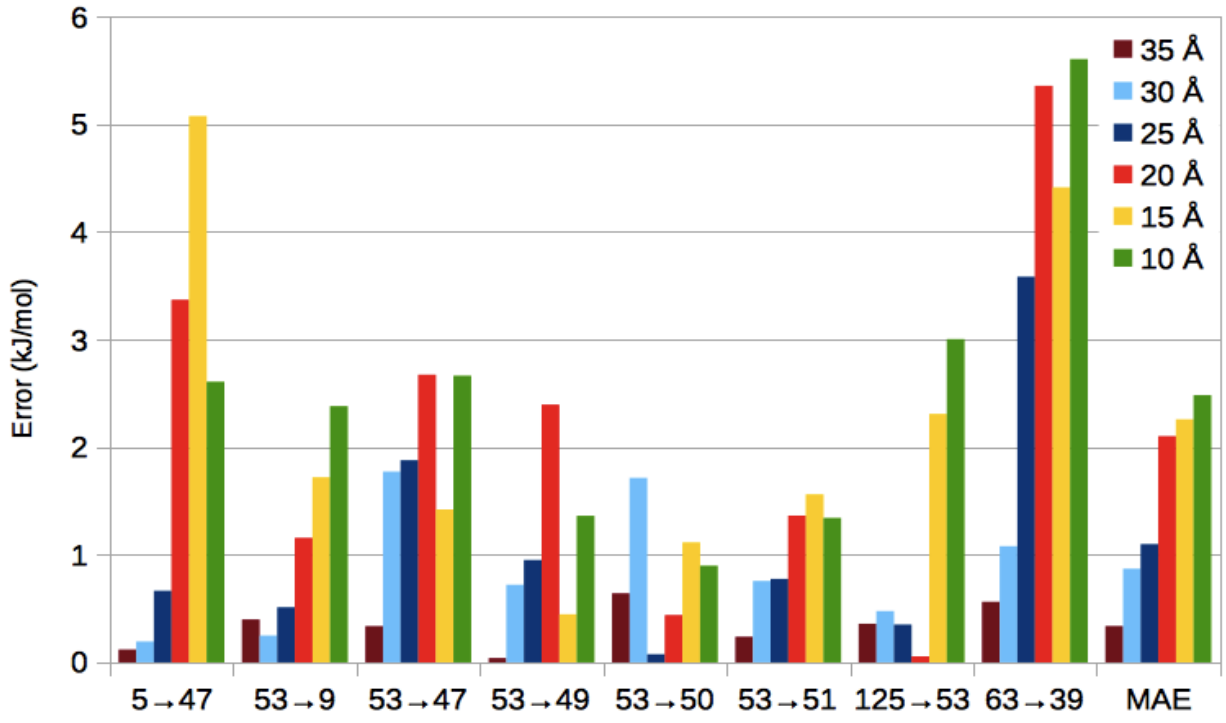

a

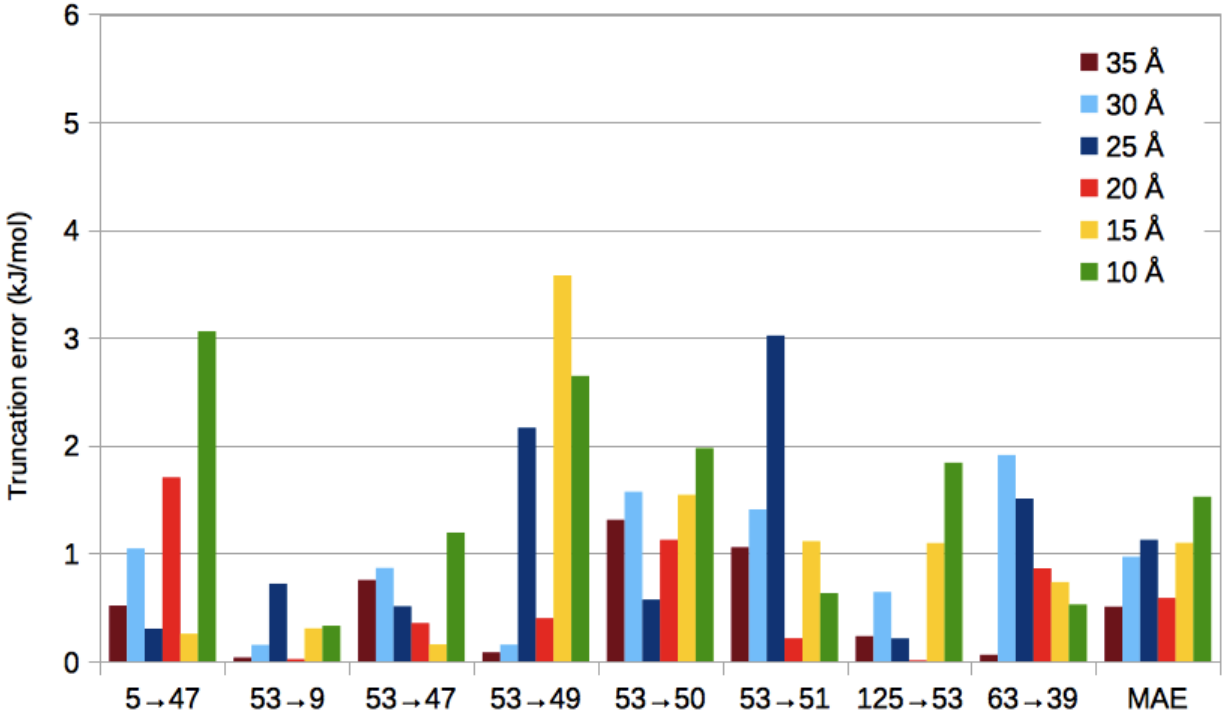

b

Figure 5. Effect of the truncation of the FEP calculations for fXa. The results are presented as the absolute difference between the full and the truncated simulation for each of the eight studied transformations. The last column shows the mean absolute error (MAE) over the eight transformations. The individual bars for the various transformations show the error for the specific cut-off radii, r. Calculations with k_{res} = (a) 4124 or (b) 1.3 kJ/mol/Å^2 (force constant for the restraint towards the starting structure for atoms between r and r – 4 Å). The uncertainties in the truncation errors are 0.3–0.8 kJ/mol.

TOC graphics